Acta Pharmaceutica Sinica B 2019;9(1):157–166

Chinese Pharmaceutical Association
Institute of Materia Medica, Chinese Academy of Medical Sciences

Acta Pharmaceutica Sinica B

www.elsevier.com/locate/apsb
www.sciencedirect.com

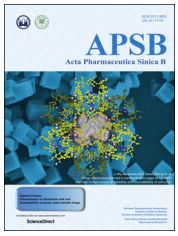

ORIGINAL ARTICLE

Pharmacometabolomic prediction of individual differences of gastrointestinal toxicity complicating myelosuppression in rats induced by irinotecan

Yiqiao Gao[a,b], Wei Li[a,b], Jiaqing Chen[a,b], Xu Wang[a,b], Yingtong Lv[a,b], Yin Huang[a,b], Zunjian Zhang[a,b,*], Fengguo Xu[a,b,]**

[a]*Key Laboratory of Drug Quality Control and Pharmacovigilance (Ministry of Education), State Key Laboratory of Natural Medicine, China Pharmaceutical University, Nanjing 210009, China*
[b]*Jiangsu Key Laboratory of Drug Screening, China Pharmaceutical University, Nanjing 210009, China*

Received 1 June 2018; received in revised form 21 August 2018; accepted 30 August 2018

KEY WORDS

Irinotecan;
Individual differences;
Complicating toxicity;
Prediction;
Metabolomics;
Gastrointestinal toxicity;
Biomarkers;
Diarrhea

Abstract Pharmacometabolomics has been already successfully used in toxicity prediction for one specific adverse effect. However in clinical practice, two or more different toxicities are always accompanied with each other, which puts forward new challenges for pharmacometabolomics. Gastrointestinal toxicity and myelosuppression are two major adverse effects induced by Irinotecan (CPT-11), and often show large individual differences. In the current study, a pharmacometabolomic study was performed to screen the exclusive biomarkers in predose serums which could predict late-onset diarrhea and myelosuppression of CPT-11 simultaneously. The severity and sensitivity differences in gastrointestinal toxicity and myelosuppression were judged by delayed-onset diarrhea symptoms, histopathology examination, relative cytokines and blood cell counts. Mass spectrometry-based non-targeted and targeted metabolomics were conducted in sequence to dissect metabolite signatures in predose serums. Eventually,

Abbreviations: AUC-ROC, area under receiver operating characteristic; BHB, β-hydroxybutyric acid; C, control group; CA, cholic acid; CPT-11, irinotecan; DBIL, direct bilirubin; DCA, deoxycholic acid; FDR, false discovery rate; GCA, glycocholic acid; IBIL, indirect bilirubin; IT-TOF/MS, ion trap/time-offlight hybrid mass spectrometry; Lys, lysine; MSTFA, *N*-methyl-*N*-trifluoroacetamide; NS, non-sensitive group; NSgt, non-sensitive for gastrointestinal toxicity; NSmt, non-sensitive for myelosuppression toxicity; OPLS-DA, orthogonal partial least-squares-discriminant analysis; PCA, principal component analysis; pFDR, false-discovery-rate-adjusted *P* value; Phe, phenylalanine; PLS-DA, partial least-squares-discriminant analysis; QC, quality control; RSD, relative standard deviation; S, sensitive group; Sgt, sensitive for gastrointestinal toxicity; Smt, sensitive for myelosuppression toxicity; T, CPT-11 treated group; Trp, tryptophan; UFLC, ultrafast liquid chromatography; VIP, variable importance in the projection

*Corresponding author at: Key Laboratory of Drug Quality Control and Pharmacovigilance (Ministry of Education), State Key Laboratory of Natural Medicine, China Pharmaceutical University, Nanjing 210009, China. Tel./fax: +86 25 83271454.

**Corresponding author at: Key Laboratory of Drug Quality Control and Pharmacovigilance (Ministry of Education), State Key Laboratory of Natural Medicine, China Pharmaceutical University, Nanjing 210009, China. Tel./fax: +86 25 83271021.

E-mail addresses: zunjianzhangcpu@hotmail.com (Zunjian Zhang), fengguoxu@gmail.com (Fengguo Xu).

Peer review under responsibility of Institute of Materia Medica, Chinese Academy of Medical Sciences and Chinese Pharmaceutical Association.

https://doi.org/10.1016/j.apsb.2018.09.006

two groups of metabolites were screened out as predictors for individual differences in late-onset diarrhea and myelosuppression using binary logistic regression, respectively. This result was compared with existing predictors and validated by another independent external validation set. Our study indicates the prediction of toxicity could be possible upon predose metabolic profile. Pharmacometabolomics can be a potentially useful tool for complicating toxicity prediction. Our findings also provide a new insight into CPT-11 precision medicine.

1. Introduction

Chemotherapy is one of the major methods for cancer therapy[1–4]. However, antitumor drugs could induce varieties of adverse effects including myelosuppression, nausea, vomiting, diarrhea and peripheral neuropathy[5–8]. What's more, these adverse effects often show large individual differences. Thus, in order to maximize drug efficacy and minimize toxicity, it is necessary to pick out the subgroups of patients with different responses.

Pharmacometabolomics is an effective approach for individual differences recognition and prediction. It was first proposed in 2006 and defined as "the prediction of the outcome (for example, efficacy or toxicity) of a drug or xenobiotic intervention in an individual based on a mathematical model of pre-intervention metabolite signatures[9]." In recent years, pharmacometabolomics has been widely used in personalized medicine[10–12] and shows great potential in drug toxicity prediction[13–15]. Almost all previous studies only focused on one specific adverse effect. However, in clinical, two or more different toxicities are always accompanied with each other, which puts forward new challenges for pharmacometabolomics.

In the current study, we try to explore the possibility of using pharmacometabolomic approach to predict two complicating toxicities using irinotecan (CPT-11) as an example. CPT-11 is a potent inhibitor of topoisomerase I[16] and has been used as first-line or second-line chemotherapeutic agents in several malignancies, especially for colorectal cancer[17]. However, the higher risk of several adverse effects and individual differences, particularly gastrointestinal toxicity (delayed-onset diarrhea, grade 3–4 occurred in 22%–44%[18–21]) complicating myelosuppression toxicity (neutropenia, leukopenia, etc., grade 3–4 occurred in 27%–54%[20–22]) have been reported, which limited its clinical application. Previous investigations indicated that genetic variations of enzymes, especially UGT1A1, which involved in CPT-11 metabolism (Supporting Information Fig. S1), play an important role in chemotherapeutic toxicity individual differences[23,24]. Thus, US Food and Drug Administration recommended the UGT1A1*28 genotyping test before CPT-11 administration. However, recent studies revealed that UGT1A1 genotyping may have limited effects on toxicity prediction. Carboxylesterases, ABC-transporters, patients living habits, etc., could all influence the individual chemosensitivity[25–30]. Meanwhile, some studies indicated that bilirubin and pharmacokinetic markers such as biliary index could also predict CPT-11 toxicity[21,31]. However, these predictors only focus on one single specific adverse effect of CPT-11 and the prediction ability remains questioned[32,33]. Thus, new indicators are needed to predict individual response to CPT-11.

In this paper, a pharmacometabolomic study was designed and performed to screen the exclusive biomarkers in predose serums which could predict late-onset diarrhea and myelosuppression of CPT-11 simultaneously. CPT-11-induced toxicity model was divided into sensitive (S) group (more deviations from control group) and non-sensitive (NS) group (closer to control group) based on non-targeted metabolomics natural grouping of postdose serum samples. The severity and sensitivity differences in gastrointestinal toxicity and myelosuppression were evaluated by delayed-onset diarrhea symptoms, histopathology examination, blood routine examination and relative cytokines, which indicated more severe chemotherapy-induced injuries happened in sensitive group (S group). Next, mass spectrometry-based non-targeted metabolomic analysis of predose serum samples was conducted to screen the potential biomarkers which can predict CPT-11-induced late-onset diarrhea and myelosuppression respectively. These biomarkers were confirmed by a follow-up targeted metabolomics using LC–MS/MS and constructed the prediction models based on the quantitative analysis results and binary logistic regression. The prediction abilities of these two models were compared with existing predictors (UGT1A1, biliary index, bilirubin) and validated by another independent external experiment.

2. Materials and methods

2.1. Chemicals and reagents

Irinotecan hydrochloride (CPT-11, active pharmaceutical ingredients) was obtained from Jaripharm (Jiangsu, China). CPT-11 for injection was prepared according to published papers[34–36]. *O*-Methoxyamine hydrochloride, *N*-methyl-*N*-trifluoroacetamide (MSTFA), pyridine, deoxycholic acid (DCA, 98%), glycocholic acid (GCA, 97%), tryptophan (Trp, 98%), lysine (Lys, 98%), phenylalanine (Phe, 99%) and cortisone acetate were purchased from Sigma–Aldrich (St. Louis, MO, USA). Cholic acid (CA, 98%), *β*-hydroxybutyric acid (BHB, 95%) were purchased from Bailingwei (Beijing, China). Cortisone acetate, fudosteine and acetaminophen were obtained from National Institutes for Food and Drug Control (Beijing, China). Camptothecin (95%), 7-ethyl-10-hydroxy-camptothecin (SN-38, 99%), SN-38 glucuronide (SN-38G, 95%) were purchased from TRC (Toronto, Canada). Acetonitrile, methanol and ethyl acetate (LC/MS grade) were obtained from Merck (Germany). Deionized water was purified by Milli-Q system (Millipore, Bedford, MA, USA).

2.2. Animal experiments and samples collection

All animal procedures were performed by the Animal Ethics Committee of China Pharmaceutical University and in accordance with the Guide for the Care and Use of Laboratory Animals. Forty-eight male Sprague–Dawley rats (SPF grade, 200 ± 10 g) were

purchased from Sino–British SIPPR/BK Lab Animal Ltd. (Shanghai, China), housed in a temperature-controlled environment (24 ± 2 °C) under 12/12h-dark/light cycle. After 1 week acclimatized with the raising condition, rats were randomly divided into CPT-11 treated group (T, $n = 40$) and control group (C, $n = 8$). Rats in CPT-11 treated group (T group) were treated with CPT-11 by intravenously (i.v.) injection *via* the tail vein with 60 mg/kg for 4 consecutive days (days 1–4). Rats in control group (C group) were received a same dose of vehicle. Every individual was monitored body weight loss daily and the score of diarrhea twice a day (9 a.m. and 9 p.m.) since day –1. Diarrhea score was assessed according to Akinobu Kurita's and Zeping Hu's studies[34,37]. Diarrhea observed within 2 h after the injection of CPT-11 was considered as acute diarrhea and observed after the final administration (occurring from day 5) was defined as late-onset diarrhea.

Blood samples on days 1 and 7 were collected for metabolomic studies and relative biochemical examination. Serum samples were collected at 0.25, 0.5, 1, 2, 4, 6, 8, 10, 12, and 14 h after CPT-11 administration on day 1 for pharmacokinetic studies. On day 7 after blood samples collection, rats were sacrificed and cecums were prepared for histological examination. All the samples were collected after a 12-h fast and stored in –80 °C until analysis. The process of samples collection was shown in Supporting Information Fig. S2.

2.3. Histopathology and biochemistry examination

Cecums were embedded in paraffin, stained by hematoxylin and eosin for histological examination. Blood cell counts (erythrocyte, leukocyte, platelet, neutrophil and lymphocyte) and bilirubin were tested in ZhongDa Hospital (Nanjing, China). Rat UGT1A1 in serums was tested by ELISA Kit (Jianglaibio, Shanghai, China). Tumor necrosis factor-α (TNF-α), interleukin-1β (IL-1β) and interleukin-6 (IL-6) were determined by Luminex 200 (Luminex, Austin, TX, USA) and Milliplex Map kit (EMD Millipore, Billerica, MA, USA).

2.4. Non-targeted metabolomics analysis

Non-targeted metabolomic analysis was performed on both GC/MS and LC/MS. For GC/MS analysis, samples were separated on an Rtx-5MS capillary column (30.0 m × 0.25 mm ID, 0.25 μm) and detected by GC/MS-QP2010 Ultra (Shimadzu Inc., Kyoto, Japan). Ultrafast liquid chromatography (UFLC) system coupled with ion trap/time-offlight hybrid mass spectrometry (IT-TOF/MS, Shimadzu Inc., Kyoto, Japan) was used to conduct LC/MS analysis. Blood sample preparation, analytical and data preprocessing methods were all on the basis of our previous studies[38,39] (as shown in Supporting Information Methods 1.1). After serum metabolomics analysis, GC/MS data and LC/MS data were combined as the whole dataset to contain as much information on metabolites as possible.

Multivariate statistical data analysis including principal component analysis (PCA) and orthogonal partial least-squares-discriminant analysis (OPLS-DA) was performed by SIMCA-P (version 13.0, Umetrics, Sweden). PCA was used to find the grouping trends of postdose samples to divide the models in S and NS group. OPLS-DA was used to find the potential biomarkers of predose samples between S and NS group. To ensure data quality, quality control (QC) samples were inserted randomly in analytical batch. The variable importance in the projection (VIP) values, nonparametric Mann–Whitney U test (SPSS Inc., Chicago, USA) with Benjamini–Hochberg false discovery rate (FDR) correction, area under receiver operating characteristic (AUC-ROC) curve (SPSS Inc., Chicago, USA) and lasso regression in the R package (http://www.r-project.org) were used to select the predictor biomarkers. The VIP value >1 indicated this metabolite showed contribution for grouping. False-discovery-rate-adjusted P values (pFDR) <0.05 can reduce the probability of false positives and indicate this metabolite is significantly differentially expressed[40]. AUC-ROC is a common evaluation parameter for classification performance and the classification performance can be considered excellent when AUC-ROC >0.9[38]. Metabolites heatmaps were performed by MultiExperiment View v4.6.1 (www.tm4.org).

2.5. Pharmacokinetic studies

The quantitative analysis of CPT-11 and its major metabolites (SN-38, SN-38G) was performed in accordance with published paper[41]. A Kinetex C18 column (50 mm × 2.1 mm, 2.6 μm, Phenomenex, Torrance, CA, USA) and a LC/MS 8040 triple-quadrupole mass spectrometer with ESI source (Shimadzu, Kyoto, Japan) were used for quantitative analysis. Pharmacokinetic parameters were estimated by DAS 3.2 (Mathematical Pharmacology Professional Committee of China, Shanghai, China). Blood sample preparation and analytical methods were shown in Supporting Information Methods 1.2.

2.6. Targeted metabolomics analysis of bile acids and ketogenic amino acids

The quantitative analysis of bile acids (CA, DCA, GCA) was performed on a ZORBAX Eclipse XDB-C18 column (150 mm × 2.1 mm, 3.5 μm, Agilent, CA, USA) and detected by a triple quadruple TSQ Quantum mass spectrometer with ESI source (Thermo Fisher, Palo Alto, CA, USA). Blood sample preparation and analytical methods were shown in Supporting Information Methods 1.3.

For ketogenic amino acids (Phe, Lys, Trp) and BHB quantitative analysis, samples were separated on a BEH HILIC column (100 mm × 2.1 mm, 1.7 μm, Waters, Ireland) and detected by a triple quadruple TSQ Quantum mass spectrometer with ESI source (Thermo Fisher, Palo Alto, CA, USA). Blood sample preparation and analytical methods were shown in Supporting Information Methods 1.4.

All the quantification methods were developed and validated in accordance with FDA guidance for Bioanalytical Method Validation (2013) (http://www.fda.gov/downloads/Drugs/GuidanceComplianceRegulatoryInformation/Guidances/UCM368107.pdf) in terms of accuracy, precision, linearity, matrix effects, extraction recovery and stability.

2.7. Construction and validation of prediction models

Binary logistic regression was applied to construct the prediction models (SPSS Inc., Chicago, USA). Probability (P) is a binary logistic regression parameter and the default cut value was 0.5. Logit (P) $= \ln(P/(1-P))$, its default cut value was 0. In the present study, logit (P) >0 was considered as S individuals and logit (P) <0 was considered as NS individuals. ROC curve was also used to evaluate the prediction ability of logit (P).

To further validate the prediction models, another independent experiments were performed. The logit (P) values were calculated according to the predose serum samples quantitative results. Based on logit (P) values of gastrointestinal toxicity prediction model, validation set ($n=25$) was classified into Sgt (sensitive for gastrointestinal toxicity) group (logit (P) >0, $n=15$) and NSgt

(non-sensitive for gastrointestinal toxicity) group (logit $(P)<0$, $n = 10$); meanwhile, validation set was divided into Smt (sensitive for myelosuppression toxicity) group (logit $(P)>0$, $n=15$) and NSmt (non-sensitive for myelosuppression toxicity) group (logit $(P)<0$, $n=10$) in accordance with logit (P) values of myelosuppression toxicity prediction model.

Next, diarrhea score and blood cell counts in the postdose samples were statistically compared. If diarrhea score showed significant difference ($P < 0.05$) between Sgt and NSgt group and blood cell counts showed significant difference ($P<0.05$) between Smt and NSmt group, the prediction ability of these two models were successfully validated.

3. Results

3.1. *Differentiating S and NS individuals*

After the administration of CPT-11, distinct differences in body weight loss, diarrhea score and blood cell counts between T group and C group were observed, which indicated the occurrence of gastrointestinal and myelosuppression toxic injuries (Supporting Information Fig. S3). PCA score plot of serum samples obtained on day 7 revealed that T group was completely separated from C group. Meanwhile, T group was naturally divided into two subgroups (Fig. 1), which were defined as non-sensitive group (NS group, more closer to C group) and S group (more deviations from C group), respectively. OPLS-DA model was constructed to further explore the differences between S and NS group (Supporting Information Fig. S4B). The good prediction power ($Q^2 > 0.5$) demonstrated that there were clear metabolic differences between these two subgroups.

3.2. *Data quality assurance for non-targeted metabolomics*

All the samples were randomly analyzed to avoid inter-batch differences. QC samples were made by pooling equal aliquot of each sample and mixed completely. To make sure the data quality, QC samples were inserted randomly in analytical batch. As shown in Supporting Information Figs. S4A and Fig. S6A, QC samples were clustered efficiently in PCA score plots. The relative standard deviation (RSD) values of all peaks in QC samples were lower than 30% and the retention time shifts were less than 0.10 min, which indicated the analytical process was stable and reliable[42]. Meanwhile, the permutation test of partial least-squares-discriminant analysis (PLS-DA) model with the same number of components as the corresponding OPLS-DA model confirmed that the performance of the OPLS-DA model was not overfitting[38] (Supporting Information Figs. S4C and Fig. S6B).

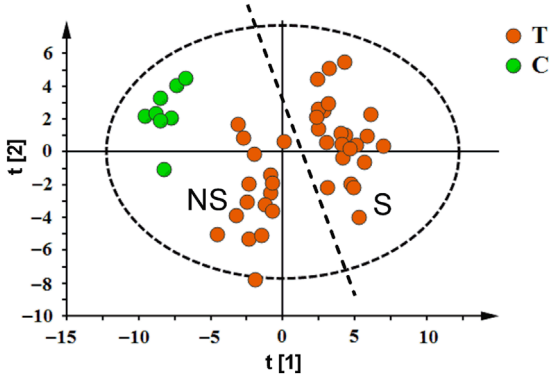

Figure 1 Recognizing individual differences after CPT-11 administration based on non-targeted metabolomic analysis of postdose serum samples. PCA score plot revealed that CPT-11 treated group (T group) was completely separated from control group (C group). T group was naturally divided into non-sensitive group (NS group) and sensitive group (S group).

3.3. *Chemotherapeutic toxicity differences verification between subgroups*

As shown in Fig. 2A and B and Supporting Information Table S4, compared with NS group, S group showed a higher late-onset diarrhea score and a lower blood cell counts (except erythrocyte counts), which indicated that S group experienced more serious injuries on gastrointestinal and myelosuppression after CPT-11 administration. Histological examination of cecums also revealed more severe damages, such as intestinal epithelium degeneration and inflammatory infiltration occurred in S group (Fig. 2C and D). TNF-α, IL-1β and IL-6 are excellent markers of inflammatory response induced by chemotherapy[43,44]. Their postdose expression levels showed significant differences between S and NS group (Fig. 2E). The baselines between S and NS group with respect to body weight (day 1), blood cell counts (day 1) and pharmacokinetic parameters of CPT-11 and its major metabolites (SN-38, SN-38G) on day 1 were also compared (Supporting Information Fig. S5 and Table S5). As a result, there were no significant differences observed. All above results confirmed the individual differences of CPT-11 chemotherapeutic toxicity.

3.4. *Screening biomarkers for prediction*

In order to find differential metabolites between S and NS group, metabolomic analysis of predose serums was performed. S and NS group were completely separated in OPLS-DA score plot with prediction power score $Q^2 > 0.5$ (Fig. 3). The corresponding PCA score plot and permutation test are shown in Supporting Information Fig. S6A and B. Twenty-seven differential metabolites were identified with VIP >1, pFDR <0.05 and AUC-ROC >0.80 (Supporting Information Table S6, Figs. S7 and S8). With AUC of late-onset diarrhea score or reduction rate of blood cell counts as the dependent variable, lasso regression was conducted to find the specific markers for predicting late-onset diarrhea and myelosuppression respectively[38,45]. Eventually, bile acids (CA, DCA, GCA) and Phe were focused as predictors for late-onset diarrhea. Meanwhile, ketogenic amino acids (Phe, Lys, Trp) could be used to predict myelosuppression.

3.5. *Establishing prediction models based on quantitative analysis results*

The absolute concentration levels of these predictive biomarkers screened out in predose serums were determined (Fig. 4A–F, Supporting Information Fig. S9). On the basis of quantitative analysis results, binary logistic regression was applied to construct the prediction models. The equation Logit $(P) = 6.190 + 1.403\text{CA} + 3.652\text{DCA} + 5.717\text{GCA} - 1.196\text{Phe}$ was used to predict CPT-11 induced late-onset diarrhea with the predictive accuracy of 95.0% in the training set ($n=40$). As shown in Fig. 4H, AUC-ROC of the model was 0.99. As for predicting myelosuppression, the predictive accuracy of equation which contained Phe, Lys and Trp was only 85.0%.

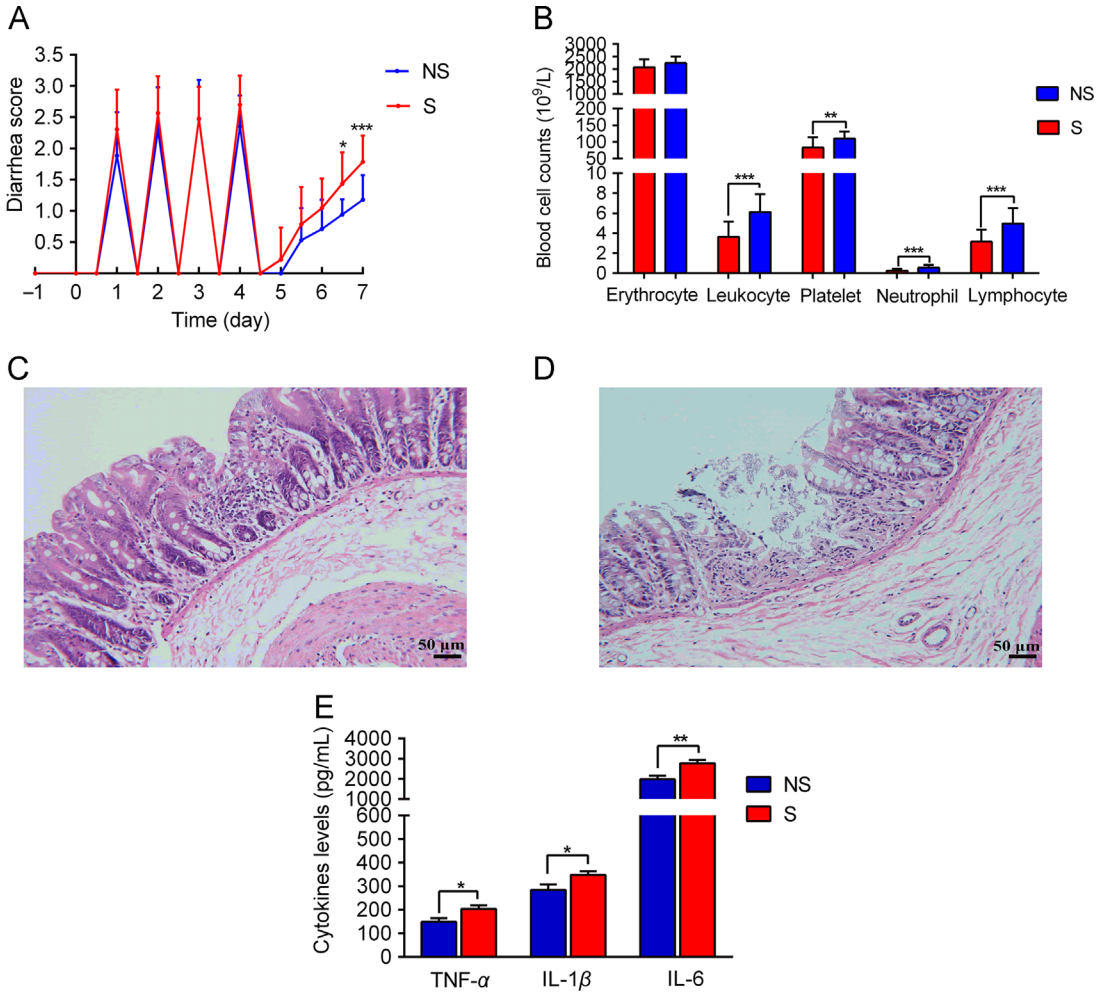

Figure 2 Chemotherapeutic toxicity differences verification between NS and S group. (A) Diarrhea scores from day –1 to day 7 in NS and S group. (B) Blood cell counts in day 7 in NS and S group. Representative histological examination of cecum in NS (C) and S (D) group (scale bar, 50 μm). (E) Cytokines (TNF-α, IL-1β and IL-6) levels in postdose serums. Data are expressed as mean ± SD. n (NS group) = 17, n (S group) = 23. Mann–Whitney U test, $^{*}P < 0.05$, $^{**}P < 0.01$, $^{***}P < 0.001$.

BHB is the common and abundant downstream metabolite of ketogenic amino acids. In clinical, it has already been used as parameter for diabetic ketoacidosis diagnosis and monitoring[46,47]. As its concentration is very low and is generally to be miss-detected by non-targeted approach, we wondered whether BHB also showed differences between S and NS groups. If so, it might be used as another variable to further improve model's accuracy. Then predose BHB concentration was also quantified (Fig. 4G) and incorporated into the prediction function. As a result, a new model Logit (P) = 66.666 − 0.075Phe − 0.054Lys–0.418Trp − 0.080BHB was constructed, which showed a higher predictive accuracy (from 85.0% to 92.5%) and higher AUC-ROC (from 0.90 to 0.99, Fig. 4I) for predicting CPT-11 induced myelosuppression in the training set (n = 40).

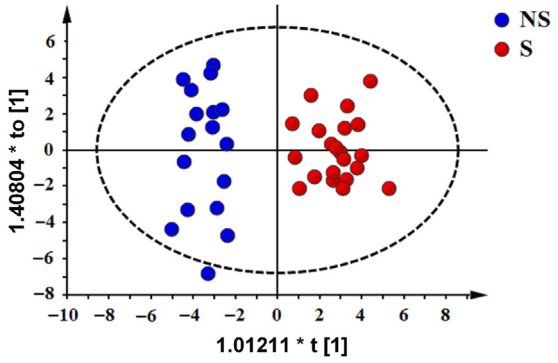

Figure 3 Screening differential metabolites between NS group and S group based on non-targeted metabolomic analysis of predose serum samples. NS and S group were completely separated in OPLS-DA score plot with prediction power score Q^2 = 0.720.

3.6. *Predictive ability comparison with existing predictors*

To illustrate the advantages of established models, the predictive ability was compared with other reported CPT-11 toxicity predictors. Biliary index is calculated based on the pharmacokinetic parameters and has been reported to be an important kinetic variable[32]. Patients with higher biliary index may experience more severe diarrhea[21,48]. Other markers derived from pharmacokinetic parameters[31] were also compared and their formulas were shown in Supporting Information Table S7. Indirect bilirubin (IBIL) can be converted into direct bilirubin (DBIL) by UGT1A1 *in vivo*. Thus DBIL could serve as a

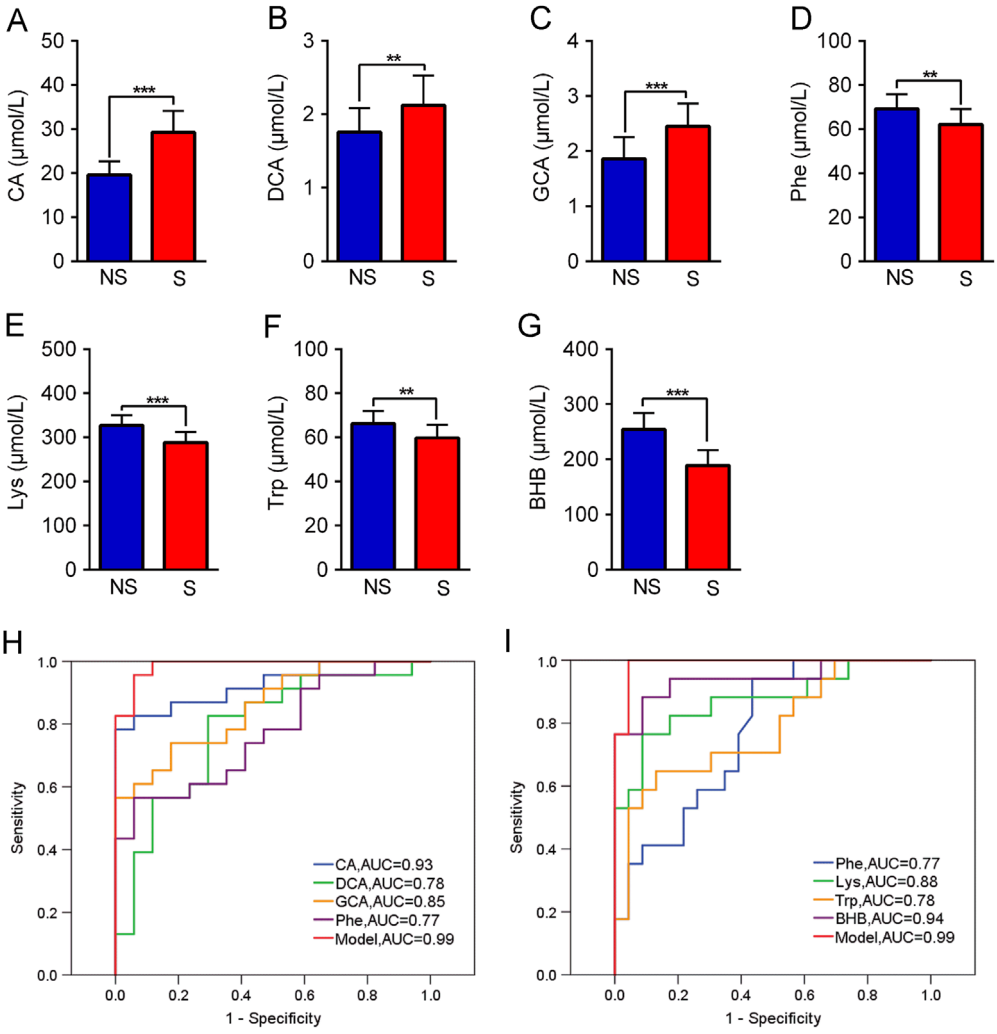

Figure 4 Targeted metabolomics analysis of screened biomarkers and prediction models construction. (A)–(G) Concentration of CA, DCA, GCA, Phe, Lys, Trp and BHB in predose serums of NS and S group, respectively. (H) ROC curves of CA, DCA, GCA, Phe and prediction model for predicting late-onset diarrhea. (I) ROC curves of Phe, Lys, Trp, BHB and prediction model for predicting myelosuppression. Data are expressed as mean ± SD. n (NS group) = 17, n (S group) = 23. Mann–Whitney U test, $^{**}P < 0.01$, $^{***}P < 0.001$. CA, cholic acid; DCA, deoxycholic acid; GCA, glycocholic acid; Phe, phenylalanine; Lys, lysine; Trp, tryptophan; BHB, β-hydroxybutyric acid.

marker for UGT1A1 activity in liver and is associated with CPT-11 induced myelosuppression[31]. We compared the correlations between CPT-11 toxicity and predictors mentioned above (Table 1 and Supporting Information Fig. S10). The results indicated the models we built showed a better correlation in predicting these two adverse effects.

3.7. *Predictive ability validation of established models*

Another independent experiment ($n=25$) was performed as validation set to further validate the predictive ability of these two established models. The levels of these selected biomarkers in predose serums were determined (Supporting Information Table S8) and logit (P) values were calculated. As described in Materials and Methods, validation set was further divided in two subgroups for CPT-11 gastrointestinal toxicity and two subgroups for CPT-11 myelosuppression toxicity according to the logit (P) values obtained using corresponding prediction model.

Diarrhea score and blood cell counts in the postdose samples were statistically compared. As shown in Fig. 5A and B, AUC of late-onset diarrhea score in Sgt group (3.55 ± 0.88, $n=15$) was significantly higher than that in NSgt group (1.53 ± 1.25, $n=10$). Meanwhile, blood cell counts (except erythrocyte counts) in Smt group ($n=15$) were significantly lower than those in NSmt group ($n=10$). The results indicated that these two models we constructed could be successfully used to predict the individual gastrointestinal and myelosuppression toxicity induced by CPT-11.

4. Discussion

Pharmacometabolomics has already been used in predicting one special toxicity of chemotherapy[13]. However in clinical practice, chemotherapy toxic effects such as diarrhea, nausea, myelosuppression usually appeared not alone[49]. Two or more different toxicities are always accompanied with each other. Different toxic

Table 1 Correlations comparison between CPT-11 adverse effects and predictors.

Predictor	*P* value	Correlation of gastrointestinal toxicity	Correlation of myelosuppression
Prediction models for gastrointestinal toxicity	$P < 0.001$	0.385	–
Prediction models for myelosuppression	$P < 0.001$	–	0.692
BI	0.002	0.340	0.302
GR	0.002	−0.252	−0.316
MR	0.027	0.019	0.053
REC	0.588	0.037	0.092
TBIL	0.766	0.063	−0.043
DBIL	0.570	−0.062	−0.220
IBIL	0.149	0.220	0.213
DBIL/IBIL	0.015	−0.313	−0.428
UGT1A1	0.034	−0.298	−0.198

BI: biliary index; GR: glucuronidation ratio; MR: metabolic ratio; REC: relative extent of conversion; TBIL: total bilirubin; DBIL: direct bilirubin; IBIL: indirect bilirubin. *P* value: Mann–Whitney U Test between NS ($n = 17$) and S group ($n = 23$). Correlation coefficients: Pearson correlation. – Not applicable.

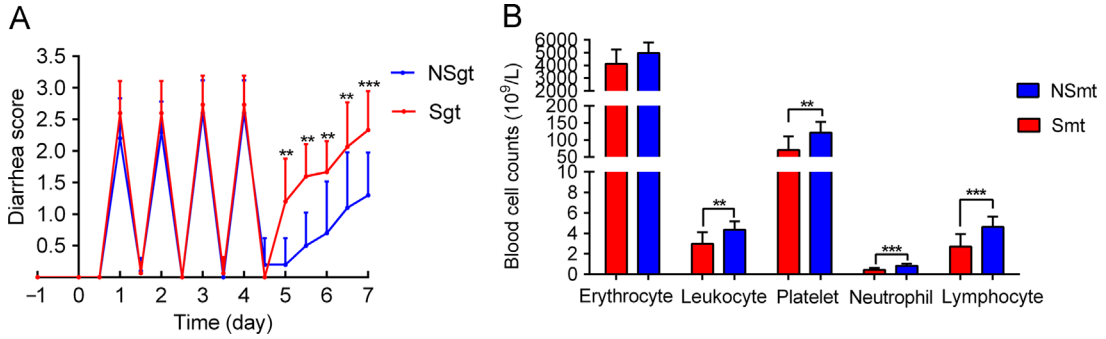

Figure 5 Validations for the predictive ability of models. (A) Diarrhea scores from day −1 to day 7 in NSgt (non-sensitive for gastrointestinal toxicity) and Sgt (sensitive for gastrointestinal toxicity) group, *n* (NSgt group) = 10, *n* (Sgt group) = 15. (B) Blood cell counts in day 7 in NSmt (non-sensitive for myelosuppression toxicity) and Smt (sensitive for myelosuppression toxicity) group, *n* (NSmt group) = 10, *n* (Smt group) = 15. Mann–Whitney U test, $^{**}P < 0.01$, $^{***}P < 0.001$.

effects have different pathogenesises and they also have cross-talk. Thus, how to pick out specific biomarkers for each type of toxicity brings new challenges for pharmacometabolomics.

In the current study, we try to explore the possibility of using pharmacometabolomic approach to predict gastrointestinal and myelosuppression toxicity caused by CPT-11. Different chemotherapy toxic effects are always accompanied with each other and have interplay of their pathogenesises. Thus, it is difficult to find a reasonable strategy in screening biomarkers which takes account of the complication's integrity and individuality. Only choosing one single toxicity as grouping criterion in screening biomarkers may ignore the interplay of chemotherapy toxicities. Treating all the pathological indexes as a whole cannot screen out specific biomarkers for specific chemotherapy toxicity.

In our studies, factors mentioned above were under consideration during data analysis. CPT-11-induced toxicity model was divided into S group and NS group based on non-targeted metabolomics natural grouping of postdose serum samples. Relative pathological indexes indicated more severe chemotherapy-induced injuries happened in S group. Then we chose toxicity scores of late-onset diarrhea or myelosuppression as the dependent variables to screen specific biomarkers for predicting gastrointestinal or myelosuppression toxicity respectively. The biomarkers we screened out *via* this strategy not only represent the overall toxicity of CPT-11, but also have more specificity in gastrointestinal or myelosuppression toxicity and closer correlations to the pathogenesises compared with the present metabolomic studies.

Non-targeted metabolomics studies of postdose serums were utilized to distinguish the individual differences of CPT-11 chemosensitivity. Based on PCA model, T group was naturally divided into S group and NS group. Furthermore, late-onset diarrhea score, blood cell counts, histological examination and cytokines test results indicated more severe chemotherapy-induced injuries happened in S group. After the verification of chemotherapeutic toxicity differences between these two subgroups, non-targeted metabolomic analysis of predose serum samples was performed and 27 differential metabolites were identified. Then we chose pathological indexes of late-onset diarrhea or myelosuppression as dependent variables in lasso regression to screen biomarkers for predicting gastrointestinal or myelosuppression toxicity, respectively. Eventually, two groups of biomarkers were screened out. These biomarkers we focused on were further confirmed by a follow-up targeted metabolomics and the absolute concentration levels of these predictive biomarkers in predose serums were

determined. Based on quantitative analysis results, binary logistic regression was applied to construct the prediction models. These two prediction models showed a good predictive ability for gastrointestinal or myelosuppression toxicity respectively in the training set ($n=40$). Finally, another independent experiment was performed as validation set ($n=25$) to further validate the predictive ability of these two established models.

As shown in Supporting Information Fig. S8 and Fig. 4, AUC-ROC values of most biomarkers were lower than those in non-targeted metabolomics studies. This phenomenon is in accordance with published study[50], which indicated it is necessary to perform targeted quantitative analysis in pharmacometabolomic studies.

After CPT-11 administration, T group was naturally divided into two subgroups. Previous studies have revealed CPT-11 can induce serum metabolic profiles changes and these changes are associated with CPT-11's toxicity[51,52]. In this study, the PCA score plot of postdose serum samples revealed S and NS groups were completely separated from C group. Comparing with NS group, S group deviated more broadly from C group. The reason for this discrepancy may due to more severe toxicity happened in S group and resulted in greater metabolic profiles changes. Pharmacometabolomic analysis of the predose serum samples revealed S and NS group were completely separated in OPLS-DA score plot. Considering about the predictive biomarkers we screened out, we speculated the individual differences in liver function, enterohepatic circulation, gut microbiota homeostasis and the levels of oxidative stress may contribute to different degrees of chemotherapeutic toxicity induced by CPT-11.

Bile acids are synthesized in liver and metabolized by the gut microbiota. CA and GCA are primarily synthesized in liver, released in intestine with bile and transported back to the liver *via* portal blood circulation, which is called "enterohepatic circulation of bile acids"[53]. Bile acids can show negative feedback effects on the bile salt export pump (BSEP)[54] and major metabolic enzymes CYP7A1 in liver by activating farnesoid X receptor[55]. Besides, GCA has already been used to evaluate liver function[56]. DCA is a secondary bile acid and mainly synthesized in intestine by gut microbiota. It has been reported that DCA can increase mucosal permeability and bacterial uptake[57]. Recent studies have revealed that bile acids can represent the metabolic interactions between gut microbiota and host[58]. Meanwhile, gut microbiota also plays an important role in pharmacokinetics of CPT-11[48] and the disturbance of gut microbiota is one of the mechanisms of chemotherapy-induced diarrhea[59,60]. Gut microbiota can also influence enterohepatic circulation and the levels of bile acids[61,62]. In our studies, CPT-11 induced late-onset diarrhea can be predicted by CA, DCA and GCA, whose different levels may represent the differences in liver function, enterohepatic circulation and homeostasis status of gut microbiota.

It should be noted that in our studies, CLs of SN-38G between NS and S group showed a significant difference (Supporting Information Table S5). As shown in Supporting Information Fig. S1, SN-38G is excreted in bile and then hydrolysed to SN-38 by gut bacterial β-glucuronidase. The difference of CLs may indicate that the gut microbiota homeostasis individual differences existed between S and NS group, which supported our speculations.

Ketogenic amino acids can be converted to ketone bodies (mainly BHB) and ultimately degraded in the citric acid cycle. Ketogenic amino acids have been reported to show efficacy in hepatosteatosis[63]. BHB has showed many signaling functions such as suppressing oxidative stress as endogenous histone deacetylase inhibitor[64,65]. Chemotherapy-induced myelosuppression has various proposed pathogenesises including oxidative stress[66]. Meanwhile, oxidative stress also contributes to the pathophysiology of CPT-11-induced chemotherapy toxicity[67]. A higher levels of Phe, Lys, Trp and BHB may enhance the ability to resist oxidative stress and further reduce myelosuppression induced by CPT-11. It should be noted that ketogenic diets have already been used in clinical studies as a complementary approach for cancer therapy to enhance curative effects[68,69]. However, it is still unclear whether ketone bodies could reduce chemotherapy toxicity as well.

From the above, we established two models to predict gastrointestinal toxicities and myelosuppression induced by CPT-11 respectively. However, in clinical, the typing, grading and staging of cancers are various. Besides, CPT-11 is always combined with other antitumor drugs such as fluorouracil for the treatment. The complicated situations in clinical practice are challenges for application of our findings and deserve further investigation and discussion.

5. Conclusions

In this study, a pharmacometabolomic approach was performed to screen exclusive predictive biomarkers for CPT-11 complicating toxicity. Eventually, the model based on CA, DCA, GCA and Phe showed a good predictive ability for late-onset diarrhea; while another model based on Phe, Lys, Trp combined with BHB showed a good predictive ability for myelosuppression. These two prediction models we established were compared with existing predictors and validated by another independent external experiment. This study demonstrates that drug toxicity could be predicted using predose metabolome. Our fingdings could provide new insight into CPT-11 complicating toxicity and may facilate personalized medicine of other antitumor drugs in future.

Acknowledgments

This study was financially supported by the NSFC (Nos. 81773861, 81773682, 81573385 and 81302733, China), Macao Science and Technology Development Fund (FDCT, No. 006/2015/A1, China), Jiangsu Six Talent Peaks Program (YY-046, China), the Program for Jiangsu Province Innovative Research (KYCX17_0681, China), a project funded by the Priority Academic Program Development of Jiangsu Higher Education Institutions (PAPD, China).

Appendix A. Supporting information

Supplementary data associated with this article can be found in the online version at https://doi.org/10.1016/j.apsb.2018.09.006.

References

1. Li D, Zhang M, Xu F, Chen Y, Chen B, Chang Y, et al. Biomimetic albumin-modified gold nanorods for photothermo-chemotherapy and macrophage polarization modulation. *Acta Pharm Sin B* 2018;**8**:74–84.
2. Shen N, Hu J, Zhang L, Zhang L, Sun Y, Xie Y, et al. Doxorubicin-loaded zein in situ gel for interstitial chemotherapy of colorectal cancer. *Acta Pharm Sin B* 2012;**2**:610–4.
3. Cui C, Merritt R, Fu L, Pan Z. Targeting calcium signaling in cancer therapy. *Acta Pharm Sin B* 2017;**7**:3–17.
4. An X, Sarmiento C, Tan T, Zhu H. Regulation of multidrug resistance by microRNAs in anti-cancer therapy. *Acta Pharm Sin B* 2017;**7**:38–51.

5. Tan XZ, Wen QC, Wang R, Chen ZK. Chemotherapy-induced neutropenia and the prognosis of colorectal cancer: a meta-analysis of cohort studies. *Expert Rev Anticancer Ther* 2017;**17**:1077–85.
6. Heo YA, Deeks ED. Rolapitant: a review in chemotherapy-induced nausea and vomiting. *Drugs* 2017;**77**:1687–94.
7. Sharma R, Tobin P, Clarke PSJ. Management of chemotherapy-induced nausea, vomiting, oral mucositis, and diarrhoea. *Lancet Oncol* 2005;**6**:93–102.
8. Cliff J, Jorgensen AL, Lord R, Azam F, Cossar L, Carr DF, et al. The molecular genetics of chemotherapy-induced peripheral neuropathy: a systematic review and meta-analysis. *Crit Rev Oncol Hematol* 2017;**120**:127–40.
9. Clayton TA, Lindon JC, Cloarec O, Antti H, Charuel C, Hanton G, et al. Pharmaco-metabonomic phenotyping and personalized drug treatment. *Nature* 2006;**440**:1073–7.
10. Everett JR, Loo RL, Pullen FS. Pharmacometabonomics and personalized medicine. *Ann Clin Biochem* 2013;**50**:523–45.
11. Everett JR. From metabonomics to pharmacometabonomics: the role of metabolic profiling in personalized medicine. *Front Pharmacol* 2016;**7**:297.
12. Nicholson JK, Wilson ID, Lindon JC. Pharmacometabonomics as an effector for personalized medicine. *Pharmacogenomics* 2011;**12**:103–11.
13. Kwon HN, Kim M, Wen H, Kang S, Yang HJ, Choi MJ, et al. Predicting idiopathic toxicity of cisplatin by a pharmacometabonomic approach. *Kidney Int* 2011;**79**:529–37.
14. Winnike JH, Li Z, Wright FA, Macdonald JM, O'Connell TM, Watkins PB. Use of pharmaco-metabonomics for early prediction of acetaminophen-induced hepatotoxicity in humans. *Clin Pharmacol Ther* 2010;**88**:45–51.
15. Coen M, Goldfain-Blanc F, Rolland-Valognes G, Walther B, Robertson DG, Holmes E, et al. Pharmacometabonomic investigation of dynamic metabolic phenotypes associated with variability in response to galactosamine hepatotoxicity. *J Proteome Res* 2012;**11**:2427–40.
16. Kunimoto T, Nitta K, Tanaka T, Uehara N, Baba H, Takeuchi M, et al. Antitumor activity of 7-ethyl-10-[4-(1-piperidino)-1-piperidino]carbonyloxy-camptothec in, a novel water-soluble derivative of camptothecin, against murine tumors. *Cancer Res* 1987;**47**:5944–7.
17. Vanhoefer U, Harstrick A, Achterrath W, Cao S, Seeber S, Rustum YM. Irinotecan in the treatment of colorectal cancer: clinical overview. *J Clin Oncol* 2001;**19**:1501–18.
18. Glimelius DB. Benefit-risk assessment of irinotecan in advanced colorectal cancer. *Drug Saf* 2005;**28**:417–33.
19. Kohne CH, de Greve GJ, Bokemeyer C, Lang I, Vergauwe P, Braumann D, et al. Capecitabine plus irinotecan *versus* 5-FU/FA/irinotecan$^{+/-}$ celecoxib in first line treatment of metastatic colorectal cancer. Safety results of the prospective multicenter EORTC phase III study 40015. *J Clin Oncol* 2005;**23**:3525.
20. Douillard JY, Cunningham D, Roth AD, Navarro M, James RD, Karasek P, et al. Irinotecan combined with fluorouracil compared with fluorouracil alone as first-line treatment for metastatic colorectal cancer: a multicentre randomised trial. *Lancet* 2000;**355**:1041–7.
21. de Man FM, Goey AK, van Schaik RH, Mathijssen RH, Bins S. Individualization of irinotecan treatment: a review of pharmacokinetics, pharmacodynamics, and pharmacogenetics. *Clin Pharmacokinet* 2018: 1–26. Available from: ⟨http://dx.doi.org/10.1007/s40262-018-0644-7⟩.
22. Nishimura T, Iwasa S, Nagashima K, Okita N, Takashima A, Honma Y, et al. Irinotecan monotherapy as third-line treatment for advanced gastric cancer refractory to fluoropyrimidines, platinum, and taxanes. *Gastric Cancer* 2017;**20**:655–62.
23. de Jong FA, de Jonge MJ, Verweij J, Mathijssen RH. Role of pharmacogenetics in irinotecan therapy. *Cancer Lett* 2006;**234**:90–106.
24. Hahn KK, Wolff JJ, Kolesar JM. Pharmacogenetics and irinotecan therapy. *Am J Health Syst Pharm* 2006;**63**:2211–7.
25. Bai Y, Wu HW, Ma X, Liu Y, Zhang YH. Relationship between *UGT1A1*6/*28* gene polymorphisms and the efficacy and toxicity of irinotecan-based chemotherapy. *Onco Targets Ther* 2017;**10**:3071–81.
26. Takano M, Sugiyama T. UGT1A1 polymorphisms in cancer: impact on irinotecan treatment. *Pharmgenomics Pers Med* 2017;**10**:61–8.
27. Cortejoso L, García MI, García-Alfonso P, González-Haba E, Escolar F, Sanjurjo M, et al. Differential toxicity biomarkers for irinotecan- and oxaliplatin-containing chemotherapy in colorectal cancer. *Cancer Chemother Pharmacol* 2013;**71**:1463–72.
28. Kweekel D, Guchelaar HJ, Gelderblom H. Clinical and pharmacogenetic factors associated with irinotecan toxicity. *Cancer Treat Rev* 2008;**34**:656–69.
29. Sunakawa Y, Ichikawa W, Fujita KI, Nagashima F, Ishida H, Yamashita K, et al. *UGT1A1*1/*28* and **1/*6* genotypes have no effects on the efficacy and toxicity of FOLFIRI in Japanese patients with advanced colorectal cancer. *Cancer Chemother Pharmacol* 2011;**68**:279–84.
30. di Martino MMMT, Arbitrio M, Leone E, Guzzi PH, Rotundo MS, Ciliberto D, et al. Single nucleotide polymorphisms of ABCC5 and ABCG1 transporter genes correlate to irinotecan-associated gastrointestinal toxicity in colorectal cancer patients: a DMET microarray profiling study. *Cancer Biol Ther* 2011;**12**:780–7.
31. Di PA, Bocci G, Polillo M, Del RM, Di DT, Lastella M, et al. Pharmacokinetic and pharmacogenetic predictive markers of irinotecan activity and toxicity. *Curr Drug Metab* 2011;**12**:932–43.
32. Cecchin E, Innocenti F, D'Andrea M, Corona G, de Mattia ME, Biason P, et al. Predictive role of the *UGT1A1*, *UGT1A7*, and *UGT1A9* genetic variants and their haplotypes on the outcome of metastatic colorectal cancer patients treated with fluorouracil, leucovorin, and irinotecan. *J Clin Oncol* 2009;**27**:2457–65.
33. Innocenti F, Undevia SD, Iyer L, Chen PX, Das S, Kocherginsky M, et al. Genetic variants in the UDP-glucuronosyltransferase 1A1 gene predict the risk of severe neutropenia of irinotecan. *J Clin Oncol* 2004;**22**:1382–8.
34. Hu Z, Yang X, Ho PCL, Chan E, Chan SY, Xu C, et al. St. John's Wort modulates the toxicities and pharmacokinetics of CPT-11 (irinotecan) in rats. *Pharm Res* 2005;**22**:902–14.
35. Trifan OC, Durham WF, Salazar VS, Horton J, Levine BD, Zweifel BS, et al. Cyclooxygenase-2 inhibition with celecoxib enhances antitumor efficacy and reduces diarrhea side effect of CPT-11. *Cancer Res* 2002;**62**:5778–84.
36. Wang X, Cui DN, Dai XM, Wang J, Zhang W, Zhang ZJ, et al. HuangQin decoction attenuates CPT-11-induced gastrointestinal toxicity by regulating bile acids metabolism homeostasis. *Front Pharmacol* 2017;**8**:156.
37. Kurita A, Kado S, Kaneda N, Onoue M, Hashimoto S, Yokokura T. Modified irinotecan hydrochloride (CPT-11) administration schedule improves induction of delayed-onset diarrhea in rats. *Cancer Chemother Pharmacol* 2000;**46**:211–20.
38. Dai D, Tian Y, Guo H, Zhang P, Huang Y, Zhang W, et al. A pharmacometabonomic approach using predose serum metabolite profiles reveals differences in lipid metabolism in survival and non-survival rats treated with lipopolysaccharide. *Metabolomics* 2016;**12**:2.
39. Zhang P, Chen J, Wang Y, Huang Y, Tian Y, Zhang Z, et al. Discovery of potential biomarkers with dose- and time-dependence in cisplatin-induced nephrotoxicity using metabolomics integrated with a principal component-based area calculation strategy. *Chem Res Toxicol* 2016;**29**:776–83.
40. Broadhurst DI, Kell DB. Statistical strategies for avoiding false discoveries in metabolomics and related experiments. *Metabolomics* 2006;**2**:171–96.
41. Corona G, Elia C, Casetta B, Toffoli G. Fast liquid chromatography-tandem mass spectrometry method for routine assessment of irinotecan metabolic phenotype. *Ther Drug Monit* 2010;**32**:638–46.
42. Naz S, Vallejo M, García A, Barbas C. Method validation strategies involved in non-targeted metabolomics. *J Chromatogr A* 2014;**1353**:99–105.
43. Gibson RJ, Bowen JM. Biomarkers of regimen-related mucosal injury. *Cancer Treat Rev* 2011;**37**:487–93.
44. Ribeiro RA, Wanderley CWS, Wong DVT, Mota JMSC, Leite CAVG, Souza MHLP, et al. Irinotecan- and 5-fluorouracil-induced intestinal mucositis: insights into pathogenesis and therapeutic perspectives. *Cancer Chemother Pharmacol* 2016;**78**:881–93.

45. Lamote K, Vynck M, Thas O, Van Cleemput J, Nackaerts K, van Meerbeeck JP. Exhaled breath to screen for malignant pleural mesothelioma: a validation study. *Eur Respir J* 2017;**50**:1700919.
46. Khalid L, Aamir AH, Livingston M, Heald A. Role of capillary ketone testing in the diagnosis and monitoring of diabetic ketoacidosis. *Int J Clin Pract* 2017;**71**:e13028.
47. Umpierrez GE, Watts NB, Phillips LS. Clinical utility of β-hydroxybutyrate determined by reflectance meter in the management of diabetic ketoacidosis. *Diabetes Care* 1995;**18**:137–8.
48. Mathijssen RH, van Alphen RJ, Verweij J, Loos WJ, Nooter K, Stoter G, et al. Clinical pharmacokinetics and metabolism of irinotecan (CPT-11). *Clin Cancer Res* 2001;**7**:2182–94.
49. Wiela-Hojeńska A, Kowalska T, Filipczyk-Cisarż E, Łapiński Ł, Nartowski K. Evaluation of the toxicity of anticancer chemotherapy in patients with colon cancer. *Adv Clin Exp Med* 2015;**24**:103–11.
50. Zhang P, Li W, Chen J, Li R, Zhang Z, Huang Y, et al. Branched-chain amino acids as predictors for individual differences of cisplatin nephrotoxicity in rats: a pharmacometabonomics study. *J Proteome Res* 2017;**16**:1753–62.
51. Wang J, Fan H, Wang Y, Wang X, Zhang P, Chen J, et al. Metabolomic study of Chinese medicine Huang Qin decoction as an effective treatment for irinotecan-induced gastrointestinal toxicity. *RSC Adv* 2015;**5**:26420–9.
52. Cui DN, Wang X, Chen JQ, Lv B, Zhang P, Zhang W, et al. Quantitative evaluation of the compatibility effects of huangqin decoction on the treatment of irinotecan-induced gastrointestinal toxicity using untargeted metabolomics. *Front Pharmacol* 2017;**8**:211.
53. Chiang JY. Regulation of bile acid synthesis: pathways, nuclear receptors, and mechanisms. *J Hepatol* 2004;**40**:539–51.
54. Meier Y, Pauli-Magnus C, Zanger UM, Klein K, Schaeffeler E, Nussler AK, et al. Interindividual variability of canalicular ATP-binding-cassette (ABC)-transporter expression in human liver. *Hepatology* 2006;**44**:62–74.
55. Trauner M, Boyer JL. Bile salt transporters: molecular characterization, function, and regulation. *Physiol Rev* 2003;**83**:633–71.
56. Ferraris R, Colombatti G, Fiorentini MT, Carosso R, Arossa W, de la Pierre MDL. Diagnostic value of serum bile acids and routine liver function tests in hepatobiliary diseases. *Dig Dis Sci* 1983;**28**:129–36.
57. Münch A, Ström M, Söderholm JD. Dihydroxy bile acids increase mucosal permeability and bacterial uptake in Human colon biopsies. *Scand J Gastroenterol* 2007;**42**:1167–74.
58. Holmes E, Kinross J, Gibson GR, Burcelin R, Jia W, Pettersson S, et al. Therapeutic modulation of microbiota-host metabolic interactions. *Sci Transl Med* 2012;**4**:137rv6.
59. Stein A, Voigt W, Jordan K. Chemotherapy-induced diarrhea: pathophysiology, frequency and guideline-based management. *Ther Adv Med Oncol* 2010;**2**:51–63.
60. Gibson RJ, Keefe DM. Cancer chemotherapy-induced diarrhoea and constipation: mechanisms of damage and prevention strategies. *Support Care Cancer* 2006;**14**:890–900.
61. Miyata M, Yamakawa H, Hamatsu M, Kuribayashi H, Takamatsu Y, Yamazoe Y. Enterobacteria modulate intestinal bile acid transport and homeostasis through apical sodium-dependent bile acid transporter (SLC10A2) expression. *J Pharmacol Exp Ther* 2011;**336**:188–96.
62. Out C, Patankar JV, Doktorova M, Boesjes M, Bos T, de Boer BS, et al. Gut microbiota inhibit Asbt-dependent intestinal bile acid reabsorption *via* Gata4. *J Hepatol* 2015;**63**:697–704.
63. Xu L, Kanasaki M, He J, Kitada M, Nagao K, Jinzu H, et al. Ketogenic essential amino acids replacement diet ameliorated hepatosteatosis with altering autophagy-associated molecules. *Biochim Biophys Acta* 2013;**1832**:1605–12.
64. Shimazu T, Hirschey MD, Newman J, He W, Shirakawa K, le Moan MN, et al. Suppression of oxidative stress by β-hydroxybutyrate, an endogenous histone deacetylase inhibitor. *Science* 2013;**339**:211–4.
65. Youm YH, Nguyen KY, Grant RW, Goldberg EL, Bodogai M, Kim D, et al. Ketone body β-hydroxybutyrate blocks the NLRP3 inflammasome-mediated inflammatory disease. *Nat Med* 2015;**21**:263–9.
66. Que L, He L, Yu C, Yin W, Ma L, Cao B, et al. Activation of Nrf2-ARE signaling mitigates cyclophosphamide-induced myelosuppression. *Toxicol Lett* 2016;**262**:17–26.
67. Rtibi K, Selmi S, Grami D, Sebai H, Amri M, Marzouki L. Irinotecan chemotherapy-induced intestinal oxidative stress: underlying causes of disturbed mucosal water and electrolyte transport. *Pathophysiology* 2017;**24**:275–9.
68. Allen BG, Bhatia SK, Buatti JM, Brandt KE, Lindholm KE, Button AM, et al. Ketogenic diets enhance oxidative stress and radio-chemotherapy responses in lung cancer xenografts. *Clin Cancer Res* 2013;**19**:3905–13.
69. Simone BA, Champ CE, Rosenberg AL, Berger AC, Monti DA, Dicker AP, et al. Selectively starving cancer cells through dietary manipulation: methods and clinical implications. *Future Oncol* 2013;**9**:959–76.